bury, 1968, edited by V. W. Hatton and S. A. Lowndes (Daresbury Nuclear Physics Laboratory, Daresbury, Lancashire, England, 1968).

[18]G. E. Fischer and Y. Murata, Nucl. Instrum. Methods 78, 25 (1970).

[19]C. K. Sinclair, private communication.

[20]R. A. Early, SLAC Technical Note No. SLAC-TN-66-15 (unpublished).

[21]W. K. H. Panofsky, in *Proceedings of the Conference on Instrumentation for High Energy Physics, Dubna, 1970*, edited by V. Z. Dzhelepov (Joint Institute for Nuclear Research, Dubna, USSR, 1971).

[22]R. M. Sternheimer, Physics 103, 511 (1956).

[23]For relativistic particles the distribution of L. Landau [J. Phys. 8, 201 (1944)], as tabulated by W. Borsch-Supan [J. Res. Natl. Bur. Stand. 65B, 245 (1961)], is used. For other particles the distribution of P. V. Vavilov, Zh. Eksp. Teor. Fiz. 32, 920 (1957) [Sov. Phys.—JETP 5, 749 (1957)], is used.

[24]D. Porat and D. Ouimette, SLAC Technical Note No. SLAC-TN-71-13 (unpublished).

[25]K. J. Kim and Y.-S. Tsai, Phys. Rev. D 8, 3109 (1973).

PHYSICAL REVIEW D VOLUME 9, NUMBER 7 1 APRIL 1974

Pion production in *pp* collisions at 102 GeV/*c**

C. M. Bromberg, D. Chaney, D. Cohen,† T. Ferbel,‡ and P. Slattery
University of Rochester, Rochester, New York 14627

J. W. Chapman, J. W. Cooper, N. Green, A. A. Seidl, and J. C. Vander Velde
University of Michigan, Ann Arbor, Michigan 48104

(Received 2 November 1973)

We present preliminary results on single-pion production and two-pion correlations making use of a 30 000-picture exposure of the ANL/NAL 30-in. hydrogen bubble chamber to 102-GeV/*c* protons. The data, when compared with those from lower energies, indicate approximate scaling of π^- production in the proton-fragmentation region, but show a continuing rise of the cross section at $y_{\text{c.m.}} = 0$. Stronger correlations are observed between pions of opposite charge than between pions of like charge. The variation with energy of the charge transferred between c.m. hemispheres is slow, as would be predicted by multiperipheral-type models.

I. INTRODUCTION

We present the results of a preliminary investigation of π^+ and π^- production in *pp* collisions at 102 GeV/*c*. The data are from the complete measurement of a sample of film containing ~650 events, plus an additional 1200 events belonging to $\leq$8-pronged topologies, which were obtained in a 30 000-picture exposure of the ANL/NAL 30-in. bubble chamber to 102-GeV/*c* protons. All tracks from these events were measured in three views using standard 2.5-μ least-count digitizing stages. A special program was written to match the tracks prior to their spatial reconstruction using the TVGP system. The inclusive spectra displayed were obtained by weighting the reconstructed events by the known topological cross sections.[1] The rapidity variable

$$y = \tfrac{1}{2}\ln\left(\frac{E+p_l}{E-p_l}\right)$$

was chosen to display the data. The rapidity of a high-momentum track is rather insensitive to momentum errors.[2] This property, coupled with the excellent pattern recognition capabilities of the 30-in. bubble chamber and its good measurement resolution for low-momentum tracks, allowed us to carry out pion rapidity measurements over the entire kinematic range available at our energy. The systematic errors for the pion rapidity spectra are dominated by corrections due to heavy-particle contamination as discussed in Sec. II.

II. SINGLE-PARTICLE SPECTRA

Corrections for K^- and $\bar{p}$ contamination in the π^- spectra, and for K^+ and high-momentum proton contamination in the π^+ spectra, were applied to the single-particle inclusive data. These corrections were made by generating, through a Monte Carlo program, $K^\pm$ spectra according to the observed K_S^0 data.[3] The energies of the generated $K^\pm$ tracks were subsequently changed by altering the mass hypothesis to be a $\pi^\pm$. These spectra were then subtracted from the measured negative and positive particle distributions. We used a K^+ (K^-) production cross section equal to 1.2 (0.8) times the observed K_S^0 cross section.[4] The $\bar{p}$ contribution was taken to be 20% of the K^- yield. Identifiable protons were removed from the data, and the high-momentum proton subtraction was determined by extrapolating the measured proton spectrum for momenta below 1.2 GeV/c (Ref. 5) in the reaction

$$pp \to p + \text{anything}. \qquad (1)$$

We assumed that the differential cross section $d\sigma/dx$ was constant for $|x|<0.8$ and equal to the value of 15 ± 3 mb observed for $-0.8 < x < -0.5$. Here x is the Feynman variable p_l^*/p_0^*, and p_l^* and p_0^* are, respectively, the longitudinal momentum of the final-state proton and the momentum of the incident protons in the center-of-mass system. We used a Monte Carlo program to generate and misinterpret the fast protons as π^+ mesons and thus corrected the positive-track spectra.

The magnitude of the corrections made to the negative spectrum were typically ~5%. The corrected π^- spectrum was observed to be symmetric about $y_{c.m.} = 0$, and was therefore folded to improve the statistics. The correction to the positive spectrum at $y_{c.m.} = 0$ was ~15%. Above $y_{c.m.} = 2$, the corrections were larger than 25%, and therefore the folding of the π^+ spectrum was restricted to $y_{c.m.} < 2$. All errors on the single-particle distributions presented contain statistical uncertainties as well as systematic uncertainties (~20% of the over-all contamination corrections).

Figure 1 displays the rapidity distributions for π^+ and π^- data, integrated over transverse momenta (p_T) and summed over all topologies. For comparison we show similar data for π^- production at 12 and 24 GeV/c.[6] The latter are plotted in terms of the laboratory rapidity (E and p_l are measured in the laboratory) in order to compare the three sets of data in the region of proton fragmentation. We note that all three π^- spectra overlap for $y_{lab} \lesssim 0.5$, at which point the higher-energy data start deviating from the 12-GeV/c and 24-GeV/c distributions. Thus the inclusive π^- cross section, for $y_{lab} < 0.5$, has apparently reached its asymptotic limit below 12 GeV/c.

In Fig. 2 we display $d\sigma/dp_T^2$ for negative particles produced in the backward hemisphere of the center-of-mass system. For comparison we show data for the same reaction at 28.5 GeV/c.[7] The growth of this

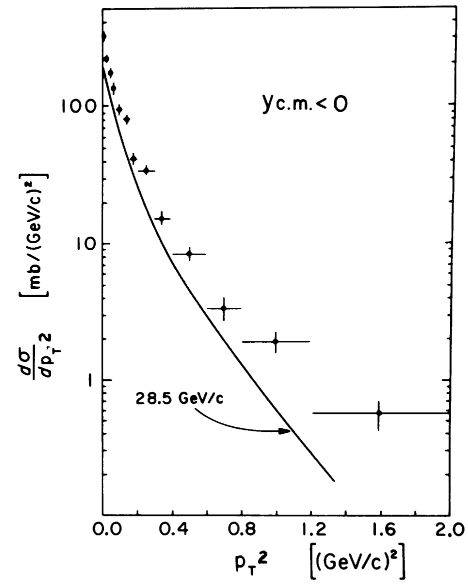

FIG. 2. The transverse momentum spectrum for all negative particles produced backward in the center-of-mass system. Also shown is a smooth curve representing the data at 28.5 GeV/c.

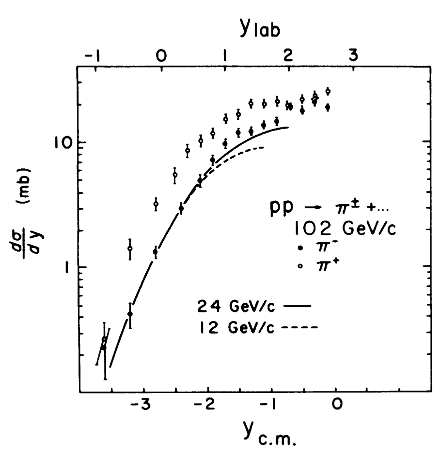

FIG. 1. The rapidity spectrum integrated over transverse momentum for π^+ and π^- mesons produced in proton-proton collisions at 102 GeV/c. Also shown are smooth curves representing data for π^- production at 12 and 24 GeV/c as a function of laboratory rapidity.

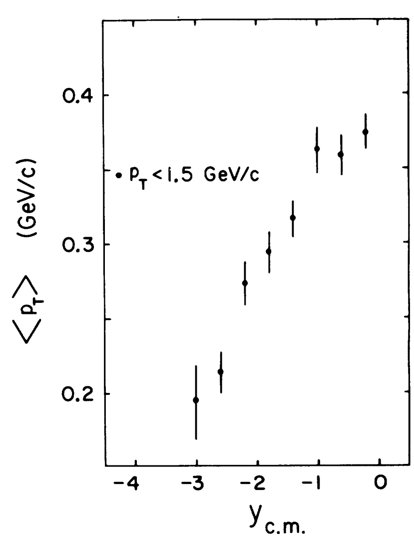

FIG. 3. The mean transverse momentum for all negative particles as a function of the rapidity in the center-of-mass system.

cross section reflects the rise of the π^- multiplicity with incident energy. However, aside from the over-all rise in the cross section, there is also an apparent change in the shape of the p_T distribution due to an additional growth of the cross section for $p_T \gtrsim 1$ GeV/c. The average value of p_T shows a slow but definite rise with energy.[8] For data in the range $p_T < 1.5$ GeV/c, we find $\langle p_T \rangle = 0.34 \pm 0.01$ GeV/c and $\langle p_T^2 \rangle = 0.17 \pm 0.01$ (GeV/c)^2. These average values were calculated using only data from the backward hemisphere to avoid possible systematic problems associated with measuring high-momentum tracks. From the measured K_S^0 spectrum (not shown), we estimate the effect of K^- contamination on these averages to be approximately $\frac{1}{2}$ the magnitude of the quoted errors.

The correlation between y and p_T is displayed in Fig. 3. The rise in $\langle p_T \rangle$ as a function of y is certainly partly due to the larger phase space available for π^- production with larger p_T values at small $y_{\rm c.m.}$, but may also have dynamical significance. The dependence of the y spectrum on multiplicity is shown in Fig. 4. The higher multiplicities are, clearly, characterized by lower mean values of $|y|$.

III. TWO-PARTICLE CORRELATIONS

In Figs. 5–7 we display data pertaining to two-particle correlations for the reactions (2)–(5):

$$pp \to \pi^c \pi^c + \cdots , \tag{2}$$

$$pp \to \pi^+ \pi^- + \cdots , \tag{3}$$

$$pp \to \pi^+ \pi^+ + \cdots , \tag{4}$$

$$pp \to \pi^- \pi^- + \cdots , \tag{5}$$

where the superscript c indicates no selection on the charge of the pion. Corrections for $K^\pm, p, \bar{p}$ contamination cannot be made in the manner that the single-particle spectra were corrected. We have, however, removed all protons identifiable by ionization, and all tracks which had a measured value for the longitudinal momentum in the center-of-mass system in excess of 4 GeV/c. This last selection removes most of the forward-produced protons while removing only a small fraction (<5%) of the forward-produced π^+. The resulting single-particle spectra are shown in Fig. 5. The remaining $K^\pm$ and $\bar{p}$ backgrounds, and the asymmetry in the positive spectra (caused by the remaining proton background), do not seriously affect the shapes or the magnitudes of the correlations to be presented.

In Figs. 6(a)–6(d) we show the double-differential cross section for reactions (2)–(5). As $|y_1|$ increases there appears to be a trend for the y_2 distribution to fall and get wider. To improve the sensitivity to small changes in the shape and magnitude of the two-particle spectra, we display in Figs. 7(a)–7(d) the correlated rapidity density for reactions (2)–(5). This density is defined as

$$R_{12} = \frac{\sigma_{\rm inel}\, d^2\sigma/dy_1 dy_2}{(d\sigma/dy_1)(d\sigma/dy_2)} - 1 \,,$$

where $\sigma_{\rm inel} = 31.9 \pm 0.8$ mb is the total inelastic cross section.[1]

The smooth curves shown in Figs. 7(a)–7(d) represent the results of a pion-production model

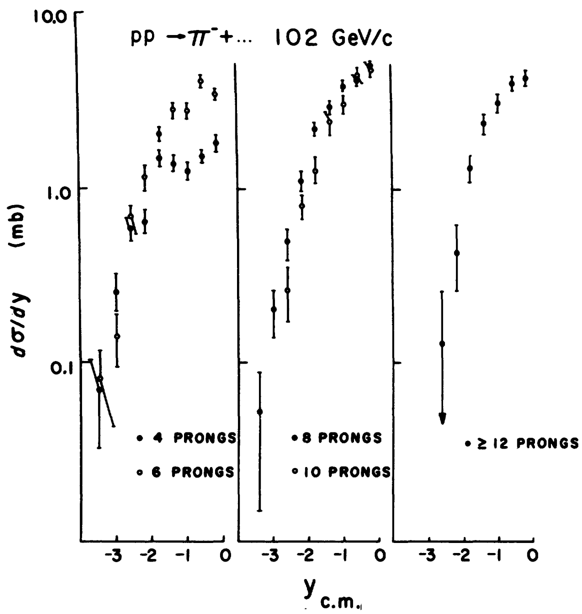

FIG. 4. The rapidity spectra for π^- mesons produced in various topological classes.

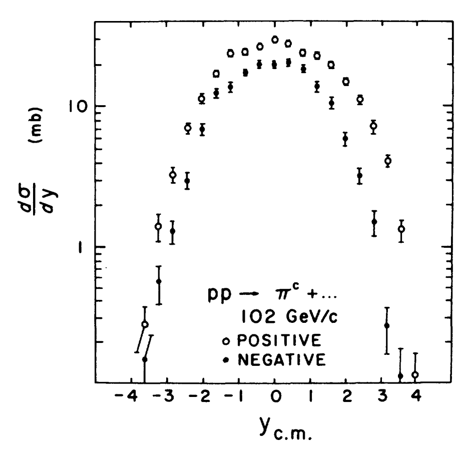

FIG. 5. The rapidity spectra for the positive and negative particles used in the calculation of the two-pion rapidity correlations. Protons have been removed using the procedure described in the text.

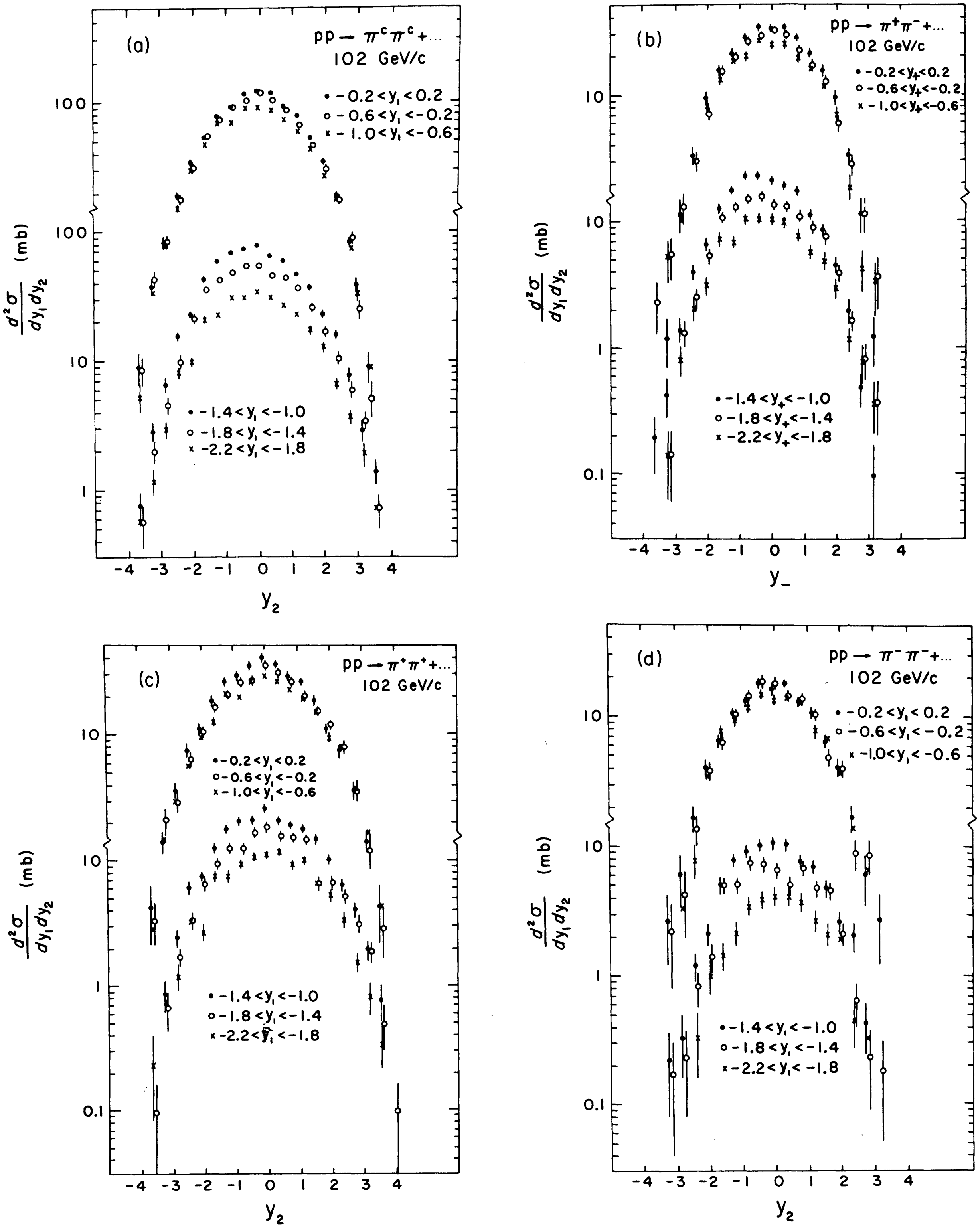

FIG. 6. The two-particle rapidity spectra in the reactions (a) $pp \to \pi^c \pi^c + \cdots$, (b) $pp \to \pi^+\pi^- + \cdots$, (c) $pp \to \pi^+\pi^+ + \cdots$, (d) $pp \to \pi^-\pi^- + \cdots$, for the rapidity intervals used in the calculation of the two-particle correlations. For clarity the data points have been displaced to the left (dark points) and to the right (open circles) of the central rapidity value in each bin.

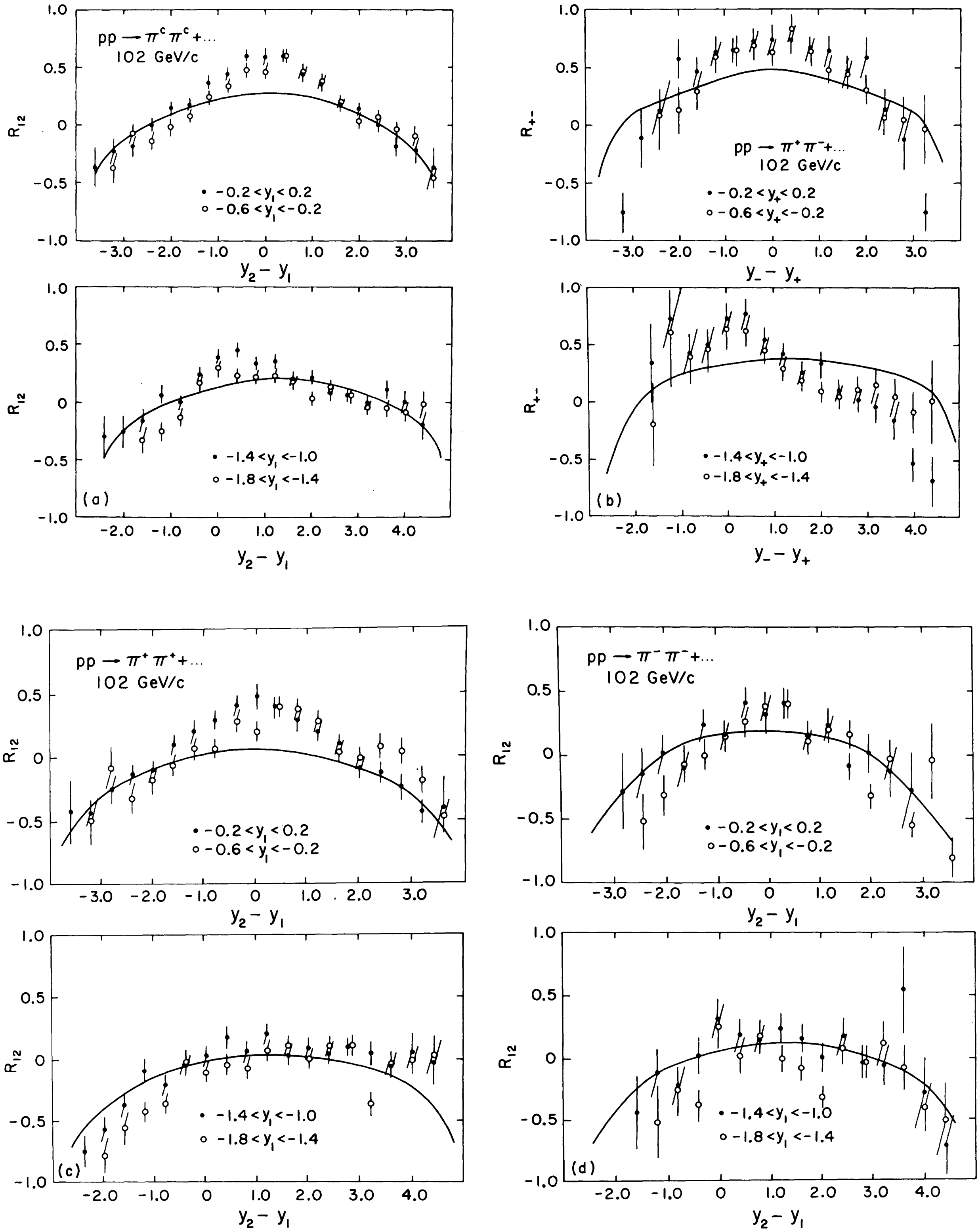

FIG. 7. The two-particle correlated rapidity density R_{12} plotted as a function of the difference between the rapidities of the two pions in the reactions (a) $pp \rightarrow \pi^c \pi^c + \cdots$, (b) $pp \rightarrow \pi^+\pi^- + \cdots$, (c) $pp \rightarrow \pi^+\pi^+ + \cdots$, (d) $pp \rightarrow \pi^-\pi^- + \cdots$. The results of the model described in the text are to be compared with the dark data points.

having the following properties:

(a) The *a priori* probabilities of each pion being a π^+, a π^-, or a π^0 are equal, as are those for each nucleon being a neutron or a proton. Charge and baryon conservation alone are used to determine which final states are possible. The probability for the production of any particular number of pions is obtained by constraining the resultant charged-particle multiplicity for the model to agree with that observed for the data.[1]

(b) The pions are produced with a cut-off transverse momentum distribution of the form $e^{-\alpha p_T^2}$, which is in approximate agreement with the data. The rapidity distribution of the generated pions is also chosen to be Gaussian in shape, with a variance which decreases with total pion multiplicity as $1/\sqrt{n}$ (also in approximate agreement with the data), and with an over-all scale factor which was chosen so that on the average the total energy carried away by all of the pions in an event amounts to $\frac{1}{2}$ the total center-of-mass energy.

In should be noted that this model is not completely devoid of correlations. For instance, the definition of R_{12} requires that

$$\iint R_{12}\frac{d\sigma}{dy_1}\frac{d\sigma}{dy_2}\,dy_1\,dy_2=f_2\sigma_{\text{inel}}{}^2\,,$$

where f_2 is the second Mueller correlation moment, and is completely determined from just the over-all multiplicity distribution which is explicitly built into the model. The intent of the model was to compare the experimental data with a "control sample" of the same general kinematic character. In addition, we wished to investigate the effect of the multiple entering of events characterizing the calculation of correlation functions such as R_{12}. Deviations from model predictions may indicate the presence of dynamical effects which would otherwise not be readily evident from just the single-particle spectra and the multiplicity distribution. The following general observations can be made.

(1) The R_{12} parameters for $\Delta y=0$ are consistently larger than expected on the basis of our model. This is true for all charge configurations. In particular, simple Mueller-Regge ideas predict the absence of $\pi^+\pi^+$ and $\pi^-\pi^-$ correlations near $y_1\approx y_2\approx 0$,[9] whereas we observe relatively large values of $R_{12}\approx 0.35$.

(2) The magnitude of R_{12} for pions of all charge [Fig. 7(a)] agrees well with that observed for the central region of pion production at 205 GeV/c (Ref. 10) and at ISR energies.[11] A similar statement can be made concerning the comparison of our results for $\pi^-\pi^-$ correlations [Fig. 7(d)] with data for the same process at 303 GeV/c.[12] Thus the maxima in R_{12} appear to be essentially energy-independent.

(3) The model does not reproduce the magnitude nor shape of R_{12}, particularily for the $\pi^+\pi^-$ data [Fig. 7(b)]. This is most evident when the two particles are produced away from the most central region [lower graph in Fig. 7(b)]. The observed correlations for $\Delta y=0$ can be taken as evidence for particle clustering in the production process, a possibility not explicitly put into our model.

Transverse-momentum correlations (the azimuth angle between transverse momenta of two particles defined as $\cos\varphi=\vec{p}_T^{\,1}\cdot\vec{p}_T^{\,2}/|\vec{p}_T^{\,1}|\,|\vec{p}_T^{\,2}|$) are shown in Fig. 8. The results are for events with six or more charged prongs. Again we note that the data for unlike-charged pions appear to show more structure than for pions of same charge. Here, however, momentum conservation requires some anticorrelation and, consequently, the lack of correlation in reactions (4) and (5), and the reduced correlation in reaction (3) for large rapidity gaps between the two pions, would appear to have a dynamic origin.[13] For example, it may be that pions of like charge frequently have other (charged

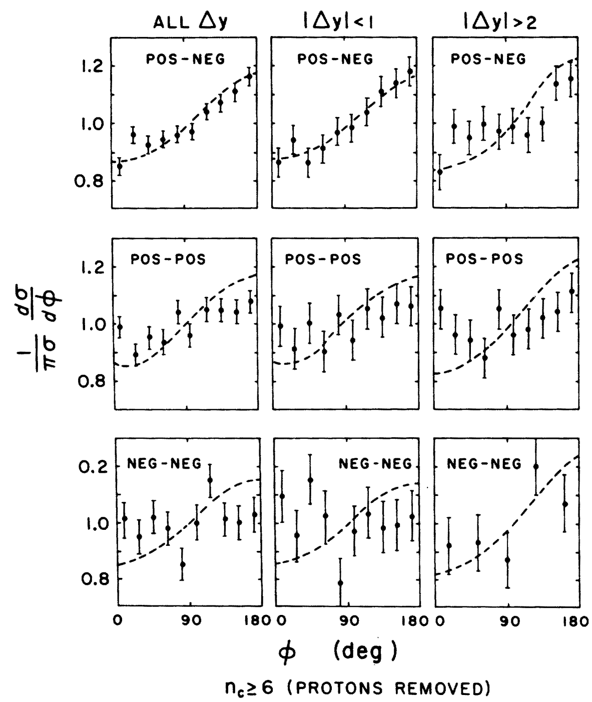

FIG. 8. The frequency for observing two pions with an angle ϕ between the transverse momenta (each plot is normalized to an average height of 1). The data are subdivided into pion charge states and into rapidity-difference intervals. The dashed curves are the results of the pion-production model described in the text. Protons and events with less than six charged particles have been removed.

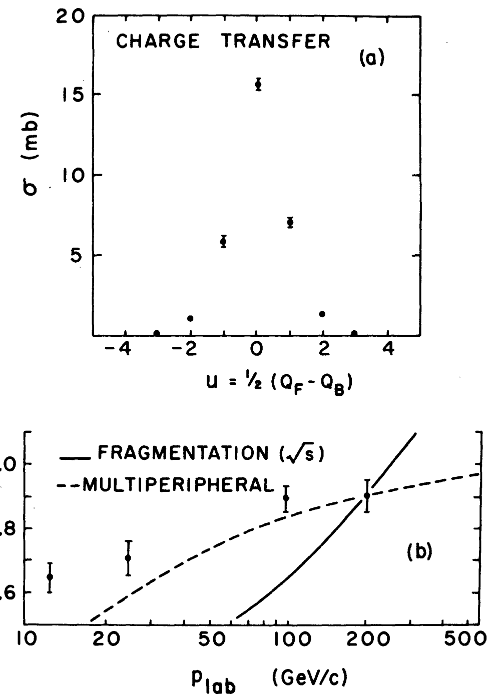

FIG. 9. (a) The cross section for observing an amount of charge u to be transferred from the backward to the forward hemisphere in the center-of-mass system, and (b) the variance of the charge-transfer distribution as a function of the incident momentum in proton-proton collisions. Also shown are predictions characterizing fragmentation and multiperipheral models (see Ref. 15).

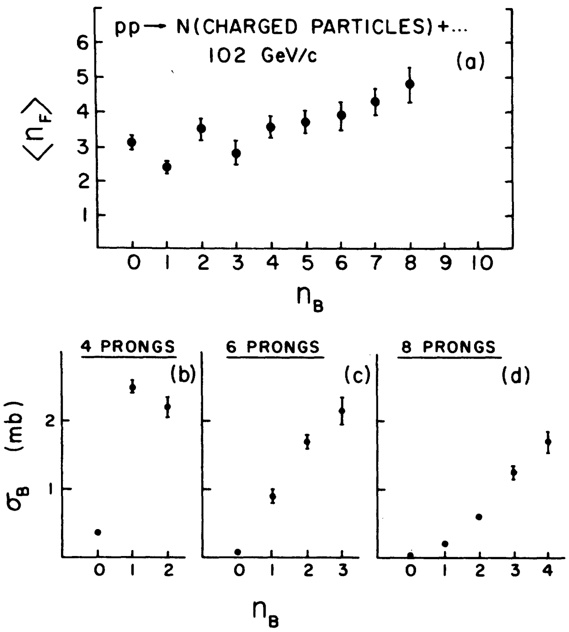

FIG. 10. (a) The mean number of charged particles observed in the forward hemisphere of the center-of-mass system $\langle n_F \rangle$ as a function of the number of charged particles observed in the backward hemisphere (n_B). (b)–(d) The cross section for observing n_B charged particles in the *backward* hemisphere of the center-of-mass system for the topological classes $N = 4, 6, 8$ prongs.

or neutral) pions between them in the rapidity chain. The diminution in the azimuthal correlation for large rapidity difference may be related to the nature of the Pomeranchuk trajectory.[14]

IV. FORWARD-BACKWARD CORRELATIONS IN THE CENTER-OF-MASS SYSTEM

The charge-transfer distribution, i.e., half the difference between the charge moving in the forward direction (Q_F) and in the backward direction (Q_B) in the center-of-mass system is shown in Fig. 9(a). (There is a very slight asymmetry in the data due to misidentification of protons.) The variance of the distribution, $\langle u^2\rangle = \frac{1}{4}\langle (Q_F - Q_B)^2\rangle$, has bearing on the nature of the production mechanism.[15] We find $\langle u^2\rangle = 0.90 \pm 0.04$. This variable has a weak dependence on laboratory momentum [Fig. 9(b)], which is more in line with predictions based on a multiperipheral mechanism (dashed curve) than with those afforded by a fragmentation or fireball model (solid curve).[15]

Finally, in Fig. 10(a) we plot the average multiplicity in the forward hemisphere $\langle n_F \rangle$ as a function of the number of particles emitted backward in the center-of-mass frame (n_B). We note that there is a weak positive correlation between n_B and $\langle n_F \rangle$ for all multiplicities. The effect of the low-multiplicity diffractive contribution is discernible in the dips observed for $n_B = 1$ and 3. In particular, the four-pronged topology exhibits a strong preference for a separation of 1 charged particle into one hemisphere of the center-of-mass system and 3 into the other [Fig. 10(b)], whereas the higher topologies [Figs. 10(c) and 10(d)] show a smooth behavior as a function of n_B.

ACKNOWLEDGMENTS

We thank the members of the NAL Neutrino Laboratory, the Accelerator Operations Group, and the Liaison Staff for aid in obtaining our film exposure. We also thank our diligent scanning and measuring personnel for their outstanding cooperation.

*Research supported in part by the U. S. Atomic Energy Commission. Computing funds at the University of Rochester are provided by the University.

†Present address: Nevis Laboratory, Columbia University, P. O. Box 137, Irvington on Hudson, New York 10533.

‡A. P. Sloan Fellow.

[1]Only about 10% of the events were not measureable in the greater than 12-pronged topologies. In the lower-multiplicity classes these losses were of the order of 3%. The full details of this analysis will be contained in C. Bromberg, Ph.D. thesis (unpublished). For the latest inelastic and topological cross sections, see C. Bromberg *et al.*, Phys. Rev. Lett. 31, 1563 (1973); 32, 83 (1974).

[2]For a more detailed discussion of the resolution attainable with the 30-in. bubble chamber see P. Slattery, in *Experiments on High Energy Particle Collisions—1973*, proceedings of the international conference on new results from experiments on high energy particle collisions, Vanderbilt University, 1973, edited by Robert S. Panvini (A.I.P., New York, 1973).

[3]See A. Seidl *et al.*, Phys. Lett. 47B, 465 (1973).

[4]These corrections tend to underestimate the K^+ contamination away from the central region of pion production. For more details see Ref. 1; J. Whitmore, in *Experiments on High Energy Particle Collisions 1973*, edited by Robert S. Panvini (Ref. 2); M. Antinucci *et al.*, Nuovo Cimento Lett. 6, 121 (1973).

[5]See J. W. Chapman *et al.*, Phys. Rev. Lett. 32, 257 (1974).

[6]H. J. Mück *et al.*, DESY Report No. F1-72/1 (unpublished). These data are statistically superior to our results and have consequently been smoothed for convenient comparison. For similar data at 205 GeV/c, see Y. Cho *et al.*, Phys. Rev. Lett. 31, 413 (1973).

[7]W. H. Sims *et al.*, Nucl. Phys. B41, 317 (1972).

[8]See for comparison the study of J. Anderson *et al.*, Phys. Lett. 45B, 521 (1973); and T. Ferbel, in proceedings of the International Symposium on High Energy Physics, Tokyo, 1973 (unpublished).

[9]See C. Quigg, in *Experiments on High Energy Particle Collisions—1973*, edited by Robert S. Panvini (Ref. 2).

[10]R. Engelmann *et al.*, ANL Report No. ANL/HEP 73-41 (unpublished).

[11]G. Bellettini, in *Proceedings of the XVI International Conference on High Energy Physics, Chicago-Batavia, Ill., 1972*, edited by J. D. Jackson and A. Roberts (NAL, Batavia, Ill., 1973), Vol. 1, p. 279.

[12]B. Y. Oh *et al.*, report from 30-in. Hybrid Spectrometer Group.

[13]For comparison see the low-energy results given in S. Stone *et al.* [Phys. Rev. D 5, 1621 (1972)] and M. C. Foster *et al.* [*ibid.* 6, 3135 (1972)].

[14]See, for example, D. Z. Freedman *et al.*, Phys. Rev. Lett. 26, 1197 (1971), and references given therein.

[15]T. T. Chou and C. N. Yang, Phys. Rev. D 7, 1425 (1973); C. Quigg and G. H. Thomas, *ibid.* 7, 2752 (1973). The curves in Fig. 9 were privately communicated to us by C. Quigg.